ARMY RESEARCH LABORATORY

Reduced Chemical-Kinetic Mechanisms for the Dark Zones of Double-Base and Nitramine Gun Propellants

by N. Ilincic, K. Seshadri,
W. R. Anderson, and N. E. Meagher

ARL-TR-1352 May 1997

The findings in this report are not to be construed as an official Department of the Army position unless so designated by other authorized documents.

Citation of manufacturer's or trade names does not constitute an official endorsement or approval of the use thereof.

Destroy this report when it is no longer need. Do not return it to the originator.

Army Research Laboratory
Aberdeen Proving Ground, MD 21005-5066

ARL-TR-1352 **May 1997**

Reduced Chemical-Kinetic Mechanisms for the Dark Zones of Double-Base and Nitramine Gun Propellants

N. Ilincic, K. Seshadri
University of California at San Diego

W. R. Anderson, N. E. Meagher
Weapons and Materials Research Directorate, ARL

Abstract

Simplified chemical-kinetic mechanisms were employed to calculate the structure of the dark zones of burning double-base and nitramine propellants. These reduced mechanisms are expected to be useful in interior ballistic calculations. First, skeletal mechanisms comprised of 22 elementary reactions among 15 species and 23 elementary reactions among 17 species were used to calculate dark zone structures for double-base and nitramine propellants, respectively. The skeletal mechanisms were previously extracted from a detailed mechanism incorporating 190 elementary reactions involving 41 species. Ignition delay times (τ_{ig}) were calculated for homogeneous mixtures in which the initial concentrations of reactants were similar to those found at the beginning of propellent dark zones. The τ_{ig} calculations were performed for various initial pressures and temperatures. The τ_{ig} calculated using the skeletal and detailed mechanisms agreed well. Reduced mechanisms were derived from the skeletal mechanisms by introducing steady-state approximations for a number of species. For double-base propellants, a reduced mechanism of three global reactions was obtained. Reduced mechanisms utilizing six and four global reactions were deduced for nitramine propellants. The τ_{ig} and structures of the dark zones calculated using the reduced three-step mechanism for double-base propellants and six-step mechanism for nitramine propellants were in agreement with calculations made using the skeletal mechanisms. Agreement using the four-step reduced mechanism for nitramine propellants was not good; however, it might still be useful for some applications.

ACKNOWLEDGMENTS

The research at the University of California at San Diego was supported by the U.S. Army Research Office through grant #ARO DAAH-95-1-0108. Dr. W. R. Anderson's travel to present this work at the Twenty-Sixth International Symposium on Combustion (July–August 1996) was partially supported by ERO (Dr. Roy Reichenbach).

The authors acknowledge S. W. Bunte, A. M. Dean, J. W. Bozzelli, R. A. Yetter, F. L. Dryer, and M. C. Lin for helpful discussions about their recent research. The authors are also grateful to J. W. Bozzelli for providing kinetic estimates for the HCN=HNC reaction.

INTENTIONALLY LEFT BLANK.

TABLE OF CONTENTS

		Page
	ACKNOWLEDGMENTS	iii
	LIST OF FIGURES	vii
	LIST OF TABLES	vii
1.	INTRODUCTION	1
2.	SKELETAL MECHANISMS	2
3.	REDUCED CHEMICAL-KINETIC MECHANISMS	6
3.1	Double-Base Propellents	8
3.2	Nitramine Propellents	10
4.	RESULTS AND DISCUSSION	12
5.	SUMMARY AND CONCLUSIONS	17
6.	REFERENCES	19
	DISTRIBUTION LIST	21
	REPORT DOCUMENTATION PAGE	25

INTENTIONALLY LEFT BLANK.

LIST OF FIGURES

Figure		Page
1.	The ratio of the difference between the rates of production and the rates of consumption to the rates of production for the species N, NH, HNO, HONO, H, OH, and O plotted as a function of time.	9
2.	The ratio of the difference between the rates of production and the rates of consumption to the rates of production for the species N_2O and NO_2 plotted as a function of time	10
3.	Profiles of temperature (T) and mole fractions of NO, N_2, CO, and CO_2 plotted as a function of time	13
4.	Profiles of temperature (T) and mole fractions of NO and N_2 plotted as a function of time	14
5.	Profile of temperature (T) and mole fractions of H_2O and HCN plotted as a function of time	14

LIST OF TABLES

Table		Page
1.	Skeletal Chemical-Kinetic Mechanisms for Modeling the Dark Zone of Double-Base and Nitramine Propellents and Associated Rate Constants	3
2.	Comparison of the Values of the Ignition Delay Times (τ_{ig}) Calculated Using the Various Mechanisms for Double-Base Propellents	7
3.	Comparison of the Values of the Ignition Delay Times (τ_{ig}) Calculated Using the Various Mechanisms for Nitramine Propellents	15
4.	Comparison of the Values of the Ignition Delay Times (τ_{ig}) Calculated Using the Various Mechanisms for Nitramine Propellents	16

INTENTIONALLY LEFT BLANK.

1. INTRODUCTION

Many double-base and nitramine propellents exhibit a two-stage flame zone during combustion. In this process, a nonluminous region separates the primary reaction zone near the surface of the propellant from the luminous secondary flame zone. The nonluminous region is commonly referred to as the dark zone. In the primary reaction zone, decomposition of the solid propellent takes place, and moderately reactive intermediate species form. These intermediate species convect away from the surface and ignite after a short delay. Recent experiments show that chemical effects caused by the use of propellents of differing chemical composition can lead to major differences in ignition delay times (τ_{ig}) during typical large-caliber gun ballistic cycles [1–4]. (The τ_{ig} in the guns are not the same as the dark-zone chemical delays.) For some propellents, these delays are undesirably long. It is believed that the range of τ_{ig} for various propellents arises from differences in the chemistry taking place in the dark zone [3, 4].

It has been established that the dark zone of solid propellents contains large amounts of NO, which is a rather weakly reactive oxidizer. The low reactivity of NO is the principal reason for the dark-zone formation. This weakly reactive mixture is rapidly converted to equilibrium products at the end of the dark zone. In particular, NO is converted to N_2, and the temperature at the end of the dark zone is much higher than at the beginning.

The temperature and species' concentrations change very slowly with distance in the dark zone. Sharp gradients in these profiles are observed only at its boundaries. It is therefore reasonable to assume that the structure of the dark zone is one-dimensional, adiabatic, and isobaric, and that diffusion of heat and mass are negligibly small.

The τ_{ig} for any reactive mixture is defined in this work as the delay time from the initiation of the reaction (time zero) to the time of maximum heat release associated with the thermal runaway. It is possible, in unusual situations, to obtain an incorrect value for τ_{ig} if there is rapid heat release from the reaction mixture that is not connected with the steep temperature gradient generated at ignition. All τ_{ig} reported in this work are compared with temperature profiles to

ensure validity of the result. Measured dark-zone thickness is directly related to the ignition delay through mass conservation and gas velocity in the dark zone [5, 6].

A detailed chemical-kinetic mechanism has been developed describing the time-dependent chemistry for reactive mixtures with initial compositions at temperature and pressure conditions similar to those at the beginning of the dark zone of double-base and nitramine propellents [7, 8] (the first-stage propellant combustion is not modeled). These reactive systems were presumed to be homogeneous, adiabatic, and isobaric. Results of calculations performed using this detailed mechanism have also been compared with experimental measurements [7, 9].

In this work, skeletal mechanisms comprising fewer elementary reactions than those in the detailed mechanisms are developed for use in modeling the structure of the dark zone of propellents. Reduced chemical-kinetic mechanisms for both propellant types are also presented. τ_{ig} were calculated under isobaric and adiabatic conditions using the skeletal and the reduced mechanisms. The results are compared with those calculated using the detailed mechanism. These calculations are done for differing values of pressure (p) and initial temperature (T^0). Pressure was held constant for all calculations.

2. SKELETAL MECHANISMS

The skeletal chemical-kinetic mechanisms employed to calculate the structure of the dark zone over the burning surface of double-base and nitramine propellents are shown in Table 1. All elementary reactions are reversible. In Table 1, the elementary reactions 1–22 among 15 species were used to model the structure of the dark zone of double-base propellents, and reactions 1–12 and 23–33 among 17 species were used to model the structure of the dark zone of nitramine propellents. These skeletal mechanisms were derived from a detailed mechanism comprising 190 elementary reactions among 41 species [9] by removing those reactions found to have negligible influence on the calculated values of the τ_{ig}. The skeletal mechanisms were used in the development of the reduced mechanisms.

Table 1. Skeletal Chemical-Kinetic Mechanisms for Modeling the Dark Zone of Double-Base and Nitramine Propellents and Associated Rate Constants

No.	Reaction		A_n	b_n	E_n
1.	$N_2O(+M)=N_2+O(+M)$ $a_0 = 1.0, a_1 = 0$ third-body efficiencies /N_2O 5.0 /H_2O 7.5 /N_2 1.0 /CO_2 3.2/	k_∞ k_0	1.26E+12 5.97E+14	0.0 0.00	62.62 56.64
2.	$HNO+NO=N_2O+OH$		8.51E+12	0.0	29.59
3.	$CO+OH=CO_2+H$		1.51E+07	1.3	-0.758
4.	$OH+H_2=H_2O+H$		2.16E+08	1.5	3.43
5.	$O+H_2=OH+H$		5.06E+04	2.67	6.29
6.	$NH+NO=N_2O+H$		3.50E+14	-0.46	0.016
7.	$N_2O+H=N_2+OH$		2.23E+14	0.0	16.75
8.	$H+HNO=NH+OH$		3.00E+14	0.0	18.00
9.	$H+HNO=H_2+NO$		4.46E+11	0.72	0.655
10.	$N_2O+NO=N_2+NO_2$		4.29E+13	0.0	47.13
11.	$HNO+HNO=N_2O+H_2O$		3.63E-03	3.98	1.19
12.	$H+NO(+M)=HNO(+M)$ $a_0 = 0.82, a_1 = 0$ third-body efficiencies /N_2O 5.0 /H_2O 5.0 /N_2 1.0 /CO_2 1.3/	k_∞ k_0	1.52E+15 8.96E+19	-0.41 -1.32	0.0 0.735
13.	$NO_2(+M)=NO+O(+M)$ $a_0 = 0.95, a_1 = -0.0001$ third-body efficiencies /N_2O 1.5 /H_2O 4.4 /N_2 1.0 /CO_2 2.3/	k_∞ k_0	7.60E+18 2.47E+28	-1.27 -3.37	73.29 74.80
14.	$NO+OH(+M)=HONO(+M)$ a_0 0.62, $a_1 = 0$ third-body efficiencies /N_2O 5.0 /H_2O 8.3 /N_2 1.0 /CO_2 1.5/	k_∞ k_0	1.988E+12 5.08E+23	-0.05 -2.51	-0.721 -0.0676

Note: Units are kilocalories, moles, seconds, and cubic centimeters. Reactions 1–22 are for double-base propellents ,and reactions 1–12 and 23–33 are for nitramine propellents.

Table 1. Skeletal Chemical-Kinetic Mechanisms for Modeling the Dark Zone of Double-Base and Nitramine Propellents and Associated Rate Constants (Continued)

No.	Reaction		A_n	b_n	E_n
15.	$H_2+NO_2=HONO+H$		3.21E+12	0.0	28.81
16.	$HNO+NO_2=HONO+NO$		6.00E+11	0.0	1.987
17.	$2OH=O+H_2O$		6.00E+08	1.3	0.0
18.	$H+OH+M=H_2O+M$ third-body efficiency /H_2O 5.0 /		1.60E+22	−2.0	0.0
19.	$NO_2+H=NO+OH$		1.30E+14	0.0	0.361
20.	$N_2O+O=NO+NO$		6.92E+13	0.0	26.60
21.	$N+NO=N_2+O$		3.27E+12	0.3	0.0
22.	$NO+H=N+OH$		1.70E+14	0.0	48.80
23.	$NH_2+NO=N_2O+H_2$		5.00E+13	0.0	24.64
24.	$CO+O+M=CO_2+M$ third-body coefficiencies /CO 1.77 /CO_2 2.7 /H_2O 5.0 /N_2O 5.0/		2.36E+15	0.0	4.34
25.	$HCN+O=NH+CO$		3.45E+03	2.64	4.98
26.	$NH_2+H=NH+H_2$		4.00E+13	0.0	3.65
27.	$NH_2+NO=N_2+H+OH$		9.30E+11	0.0	0.0
28.	$NH_2+NO=N_2+H_2O$		2.00E+20	−2.6	0.924
29.	$HNC+O=NH+CO$		5.44E+12	0.0	0.0
30.	$HNC+OH=HNCO+H$		2.80E+13	0.0	3.696
31.	$HNCO+H=NH_2+CO$		2.25E+07	1.7	3.80
32.	$CO+NO_2=NO+CO_2$		9.04E+13	0.0	33.78
33.	$HCN+M=HNC+M$		4.36E+26	−3.34	50.194

Note: Units are kilocalories, moles, seconds, and cubic centimeters. Reactions 1–22 are for double-base propellents ,and reactions 1–12 and 23–33 are for nitramine propellents.

For each elementary reaction (n), Table 1 presents the values of the frequency factor (A_n), the temperature exponent (b_n), and the activation energy (E_n) that appear in the parametric expression $k_n = A_n T^{b_n} \exp[-E_n/(\hat{R}T)]$ for the specific reaction rate constant (k_n) where $\hat{R}$ represents the universal gas constant and T, the gas temperature. The symbol M (in reactions 1, 12, 13, 14, 18, 24, and 33) represents any third body, and the catalytic efficiencies (η_i) of various species (i) acting as the third body in these reactions are shown. The catalytic efficiency of those species omitted in Table 1 is assumed to be unity. The concentration of the third body, (C_M) is calculated from the expression $C_M = [p/(\hat{R}T)] \Sigma_{i=1}^{N} X_i \eta_i$, where X_i is the mole fraction of species i. The rates of the elementary reactions 1, 12, 13, and 14 depend on pressure and are calculated using the expression [10] $k = F \cdot k_\infty \cdot k_L$, where $k_L = k_0 C_M/(k_\infty + k_0 C_M)$, $\log_{10} F = \log_{10} F_C / \{1 + [\log_{10}(k_0 C_M/k_\infty)]^2\}$, $F_C = a_0 + a_1 T$. The values of k_∞, k_0, a_0, and a_1 are shown in Table 1.

The dark zones of typical double-base propellents are known to include large amounts of NO, CO, H_2, N_2, H_2O, and CO_2 [6, 11]. Traces of CH_4 and C_2H_4 have also been observed. In addition to these species, large amounts of HCN and trace amounts of N_2O are also observed in the dark zones of common nitramine propellents [6]. Calculations with the detailed chemical-kinetic mechanisms have shown that the trace amounts of CH_4 and C_2H_4 have negligible influence on the τ_{ig} [8]. Inclusion of their chemistry would unnecessarily complicate the skeletal mechanisms. Therefore, these species are omitted from the initial mixture. The main difference between the skeletal mechanism for double-base and nitramine propellents is the inclusion of HCN chemistry in the latter. Typical conditions of interest are values of p between 1–30 atm and values of T^0 between 1,000–1,800 K. This range of values for p and T^0 was used to guide the choice of reactions in the detailed and skeletal mechanisms and the initial conditions for the numerical problem described.

Computations were performed using the SENKIN computer code written at Sandia National Laboratories [12]. A minor modification was made to the code to allow input of the functional form for pressure-dependent rate constants (presented earlier) used by Tsang and Herron [10]. A number of chemical details of the solutions from SENKIN were investigated using a

postprocessing code written at the U.S. Army Research Laboratory (ARL) [13]. Heat-release rate, chemical pathways, and logarithmically normalized sensitivities of the calculated species and temperature profiles to the rate constants were obtained in this manner. The temperature sensitivities were quite useful because these qualitatively reflect the sensitivity of the calculated τ_{ig} to the various rate coefficients (information not directly available). The pathway and sensitivity analyses were used to identify those reactions that have a significant influence on the solution, indicating which must be retained in the skeletal mechanisms.

The approximations introduced in the numerical model of the structure of the dark zone are described in detail elsewhere [5, 9]; therefore, only a brief description is given here. The system is considered to be spatially homogeneous, adiabatic, and isobaric. Calculations were performed with the initial mole fractions of NO, CO, H_2, N_2, H_2O, and CO_2 set equal to 0.24, 0.33, 0.08, 0.04, 0.20, and 0.10, respectively, for double-base propellents. For nitramine propellents, the initial mole fractions of NO, CO, H_2, N_2, H_2O, CO_2, N_2O, and HCN were set equal to 0.13, 0.22, 0.07, 0.06, 0.20, 0.09, 0.02, and 0.22, respectively. The results presented in Table 2 demonstrate that τ_{ig} calculated using the skeletal mechanism agrees very well with the values obtained from calculations using the detailed mechanism [8] for the double-base propellents. Values of τ_{ig} calculated for the nitramine propellents using the skeletal mechanism are in good agreement with those of the detailed mechanism [8]. (There are differences with those in reference 8 due to minor revisions of the detailed mechanism).

3. REDUCED CHEMICAL-KINETIC MECHANISMS

Procedures for deriving reduced chemical-kinetic mechanisms are described in detail elsewhere [14, 15]. The skeletal mechanisms were reduced by introducing steady-state approximations for a number of species. For any species, the time derivative of its concentration is the difference between production and consumption rates for that species. A steady-state approximation is justified if either the species' production or consumption rate, which of course are nearly equal at steady-state, is much larger than the time derivative of its concentration [16].

Table 2. Comparison of the Values of the Ignition Delay Times (τ_{ig}) Calculated Using the Various Mechanisms for Double-Base Propellents

Initial Conditions (atm; K)	Detailed Mechanism (41 sp., 190 r.) (s)	Skeletal Mechanism (15 sp., 22 r.) (s)	Reduced Mechanism (3 steps) (s)
1; 1,000	52.29	51.47	50.49
1; 1,400	1.035	1.046	1.042
1; 1,800	$3.738 \cdot 10^{-2}$	$3.843 \cdot 10^{-2}$	$3.684 \cdot 10^{-2}$
5; 1,000	8.297	8.062	7.769
5; 1,400	$1.142 \cdot 10^{-1}$	$1.147 \cdot 10^{-1}$	$1.142 \cdot 10^{-1}$
5; 1,800	$7.517 \cdot 10^{-3}$	$7.774 \cdot 10^{-3}$	$7.624 \cdot 10^{-3}$
10; 1,000	3.994	3.887	3.725
10; 1,400	$4.383 \cdot 10^{-2}$	$4.375 \cdot 10^{-2}$	$4.346 \cdot 10^{-2}$
10; 1,800	$3.448 \cdot 10^{-3}$	$3.571 \cdot 10^{-3}$	$3.503 \cdot 10^{-3}$
30; 1,000	1.274	1.255	1.194
30; 1,400	$9.90 \cdot 10^{-3}$	$9.75 \cdot 10^{-3}$	$9.63 \cdot 10^{-3}$
30; 1,800	$9.31 \cdot 10^{-4}$	$9.64 \cdot 10^{-4}$	$9.49 \cdot 10^{-4}$

Note: The initial mole fractions of NO, CO, H_2, N_2, H_2O, and CO_2 are set equal to 0.24, 0.33, 0.08, 0.04, 0.20, and 0.10, respectively.

For the reduced mechanisms, the concentrations of the steady-state species were calculated using the nonlinear algebraic equations resulting from the differential rate equations for these species by making the steady-state assumptions. That is, algebraic equations are obtained simply by setting these species' concentration time derivatives to zero. The steady-state species' concentrations are then specified in terms of the other species' concentrations. However, the initial steady-state species' concentrations are no longer arbitrary. For example, setting them to zero is internally inconsistent. This causes numerical difficulties. In the calculations with the reduced mechanisms, the steady-state species' initial concentrations were therefore first calculated numerically using the algebraic equations. For all cases investigated, the initial

steady-state species' concentrations were found to be negligibly small and have no significant influence on the calculated τ_{ig}.

3.1 Double-Base Propellents. In Figure 1, the ratios of the time derivatives of concentration to production rates for N, NH, HNO, HONO, H, OH, and O are plotted as a function of time (t). The calculations were performed using the skeletal mechanism for double-base propellents for p = 5 atm and T^0 = 1,400 K. Figure 1 reveals that at all conditions, except those close to t = 0 and t = τ_{ig}, the value of this ratio is very small. Therefore, it is reasonable to introduce steady-state approximations for these species. In Figure 2, the ratios of the time derivatives of concentration to production rates for N_2O and NO_2 are plotted as a function of time. These results were also obtained using the skeletal mechanism for double-base propellents for p = 5 atm and T^0 = 1,400 K. Comparison of the results in Figure 2 with the results in Figure 1 indicates that the concentration of N_2O is not in steady-state, but it is still reasonable to introduce a steady-state approximation for NO_2. In view of the results presented in Figures 1 and 2, steady-state approximations are introduced for N, NH, HNO, HONO, H, OH, O, and NO_2. The steady-state relations provide eight nonlinear algebraic equations used to calculate the concentration of the steady-state species in terms of the concentrations of the remaining species. The source terms of the species that are not in steady state are rearranged and collected in three groups, such that each group represents the rate of one of the three overall steps of the reduced mechanism, which is written as

$$2\,NO + H_2 \rightleftharpoons N_2O + H_2O, \quad I$$

$$N_2O + H_2 \rightleftharpoons N_2 + H_2O, \quad II$$

and

$$CO + H_2O \rightleftharpoons CO_2 + H_2. \quad III$$

The rates of the overall steps w_k, k = I, II, III expressed in terms of the rates of the elementary reactions are

$$
\left.
\begin{aligned}
w_I &= w_2 + w_8 + w_{11} - w_{20} + w_{22}, \\
w_{II} &= w_1 - w_7 + w_{10} + w_{22}, \\
\text{and} \\
w_{III} &= w_3,
\end{aligned}
\right\} \qquad (1)
$$

where w_n is the net reaction rate of the elementary reaction n shown in Table 1.

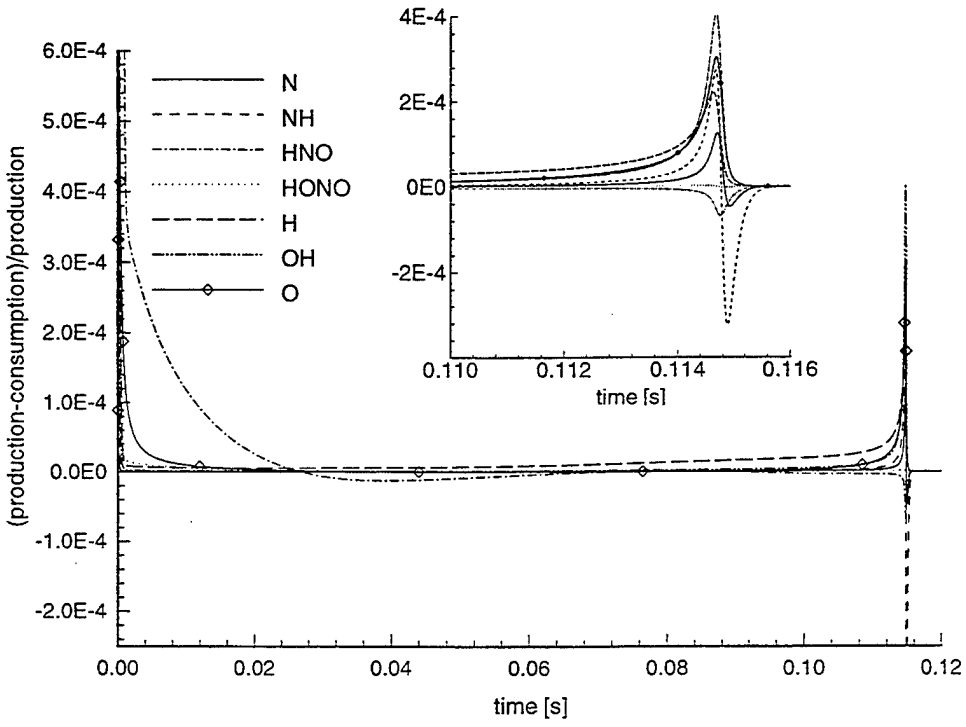

Figure 1. The ratio of the difference between the rates of production and the rates of consumption to the rates of production for the species N, NH, HNO, HONO, H, OH, and O plotted as a function of time. The calculations are performed using the skeletal mechanism for double-base propellents for p = 5 atm and T^0 = 1,400 K.

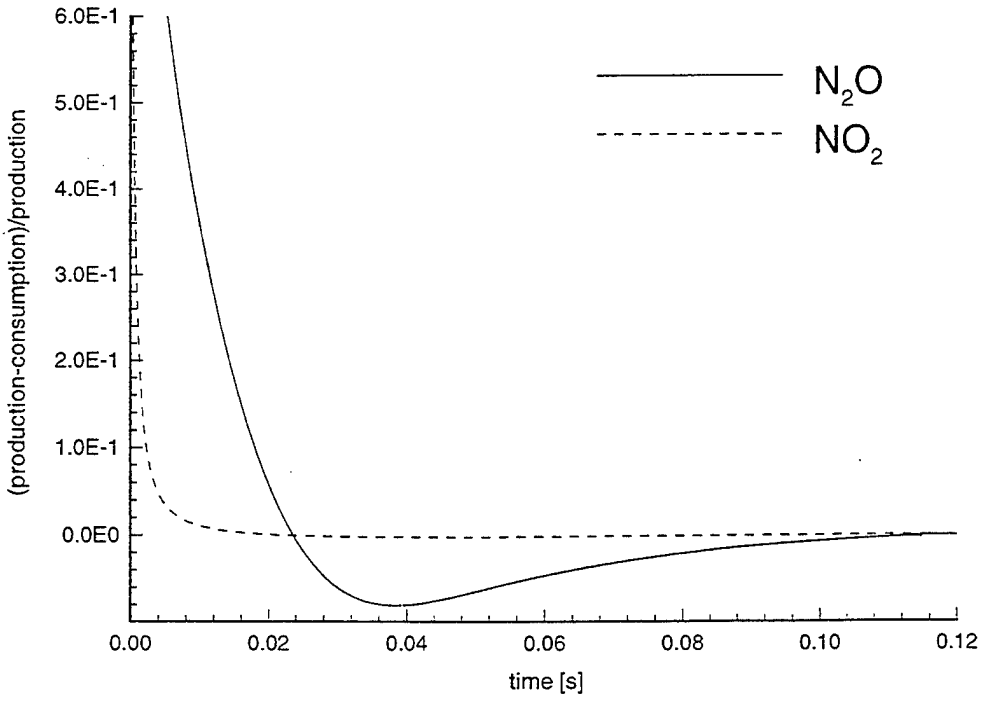

Figure 2. The ratio of the difference between the rates of production and the rates of consumption to the rates of production for the species N_2O and NO_2 plotted as a function of time. The calculations are performed using the skeletal mechanism for double-base propellents for p = 5 atm and T^0 = 1,400 K.

3.2 Nitramine Propellents. Reduced chemical-kinetic mechanisms for nitramine propellents were obtained using the same procedure employed for double-base propellents. The rates of production and consumption of various species were calculated using the skeletal mechanism for nitramine propellents. The results of these calculations demonstrate that it is reasonable to introduce steady-state approximations for NH, HNO, HNC, NH_2, NO_2, OH, and O. The steady-state assumptions provide seven nonlinear algebraic equations that can be used to calculate the concentrations of the steady-state species in terms of the concentration of the remaining species. The reduced mechanism has six overall steps, which can be written as

$$2\,NO + 2\,H_2 \rightleftharpoons N_2O + 2\,H + H_2O, \qquad \text{I}$$

$$H_2O + HCN \rightleftharpoons H_2 + HNCO, \qquad \text{II}$$

$$N_2O + 2\,H_2 \rightleftharpoons N_2 + 2\,H + H_2O, \qquad \text{III}$$

$$CO + H_2O \rightleftharpoons CO_2 + H_2, \qquad \text{IV}$$

$$2\,H + M \rightleftharpoons H_2 + M, \qquad \text{V}$$

and

$$NO + H + HNCO \rightleftharpoons N_2O + CO + H_2. \qquad \text{VI}$$

The rates of the overall steps w_k, k = I–VI expressed in terms of the rates of the elementary reactions are

$$\left.\begin{aligned} w_I &= w_2 + w_8 + w_{11}, \\ w_{II} &= w_{25} + w_{33}, \\ w_{III} &= w_1 + w_7 + w_{27} + w_{28} + w_{32}, \\ w_{IV} &= w_3 + w_{24} + w_{32}, \\ w_V &= w_7 + w_{12} + w_{24} + w_{28}\, w_{32}, \end{aligned}\right\}$$

and

$$\left.\begin{aligned} w_{VI} &= w_{25} + w_{29} + w_{31}, \end{aligned}\right\} \qquad (2)$$

To further simplify the mechanism, steady-state approximations were introduced for the species H and HNCO yielding four overall steps, which can be written as

$$2\,NO + H_2 \rightleftharpoons N_2O + H_2O, \qquad \text{I}'$$

$$NO + H_2O + HCN \rightleftharpoons N_2O + CO + 1.5\,H_2, \qquad \text{II}'$$

$$N_2O + H_2 \rightleftharpoons N_2 + H_2O, \qquad \text{III}'$$

and

$$CO + H_2O \rightleftharpoons CO_2 + H_2. \qquad \text{IV}'$$

The rates of the overall steps of the four-step mechanism w_k, k = I′–IV′ are identical to the rates for the overall steps I–IV in the six-step mechanism shown in equation 2.

4. RESULTS AND DISCUSSION

Calculations with the reduced mechanisms were performed by multiplying time derivative terms in the differential equations for the steady-state species by a small number. In the limiting case where the value of this number is zero, the differential equations are transformed to algebraic equations. The value of the multiplier was chosen such that any further decrease in its value had no influence on τ_{ig}.

In Figure 3, the profiles of temperature (T) and the mole fractions of NO, N_2, CO, and CO_2 are plotted as a function of time. The calculations were performed using the skeletal mechanism and the reduced three-step mechanism for double-base propellents for p = 5 atm and T^0 = 1,400 K. The profiles from the reduced mechanism agree closely with those calculated using the skeletal mechanism, except for times close to ignition. The maximum value of temperature and the final values of the mole fractions of various species after ignition calculated with the reduced mechanism differ from those calculated using the skeletal mechanism. These differences occur because the concentrations of the steady-state species are not included in the atom-conservation equations in calculations with the reduced mechanism. The concentrations of the steady-state species represent excess mass in the system. Therefore, in the calculations with the reduced mechanism, the mass fractions of the various atoms change with time and the final mass fractions of these atoms are different from their initial values. However, these differences become noticeable only at times close to τ_{ig}. In fact, calculations prove that the differences between the initial mass fractions of the atoms and their mass fractions at times approximately 90% of τ_{ig} are very small.

Figure 4 shows profiles of temperature (T) and the mole fractions of NO and N_2 plotted as a function of time. Figure 5 shows profiles of T and mole fractions of H_2O and HCN. These profiles are calculated using the skeletal mechanism and the reduced six-step and four-step mechanisms for nitramine propellents for p = 10 atm and T^0 = 1,400 K. The profiles in Figures 4 and 5 calculated using the reduced mechanisms agree closely with those calculated using the skeletal mechanism, except close to ignition.

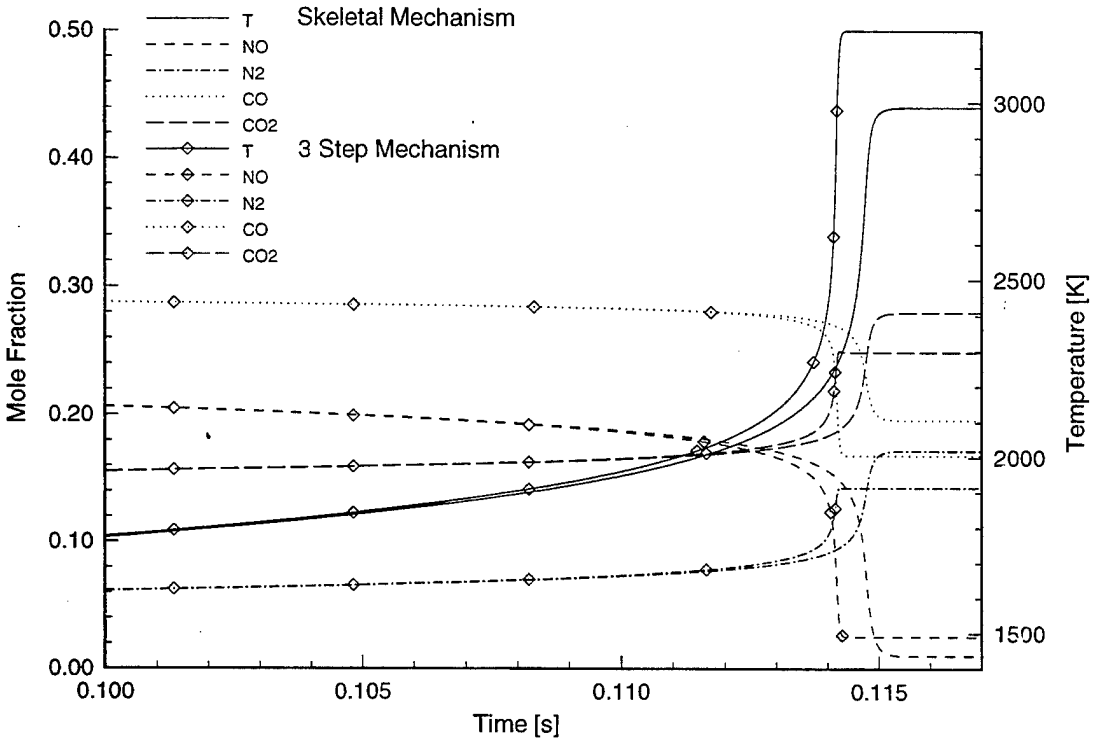

Figure 3. Profiles for temperature (T) and mole fractions of NO, N_2, CO, and CO_2 plotted as a function of time. The calculations are performed using the skeletal mechanism and the reduced three-step mechanism for double-base propellents for p = 5 atm and T^0 = 1,400 K.

Table 2 shows that the values of the τ_{ig} calculated using the reduced three-step mechanism for double-base propellents agree well with those calculated using the skeletal mechanism. The differences in the values of τ_{ig} are less than 10%, with τ_{ig} from the reduced mechanism smaller than that obtained using the skeletal mechanism. If a steady-state approximation is introduced for N_2O, a reduced two-step mechanism is obtained. The value of τ_{ig} calculated using this two-step mechanism at p = 1 atm and T^0 = 1,000 K is found to be 50% lower than calculated with the three-step mechanism. This result illustrates that a steady-state approximation for N_2O is not justified (although at other conditions the agreement is better).

Table 3 compares the values of the τ_{ig} calculated using the six-step and four-step mechanisms for nitramine propellents with those calculated using the skeletal mechanism. The values of τ_{ig}

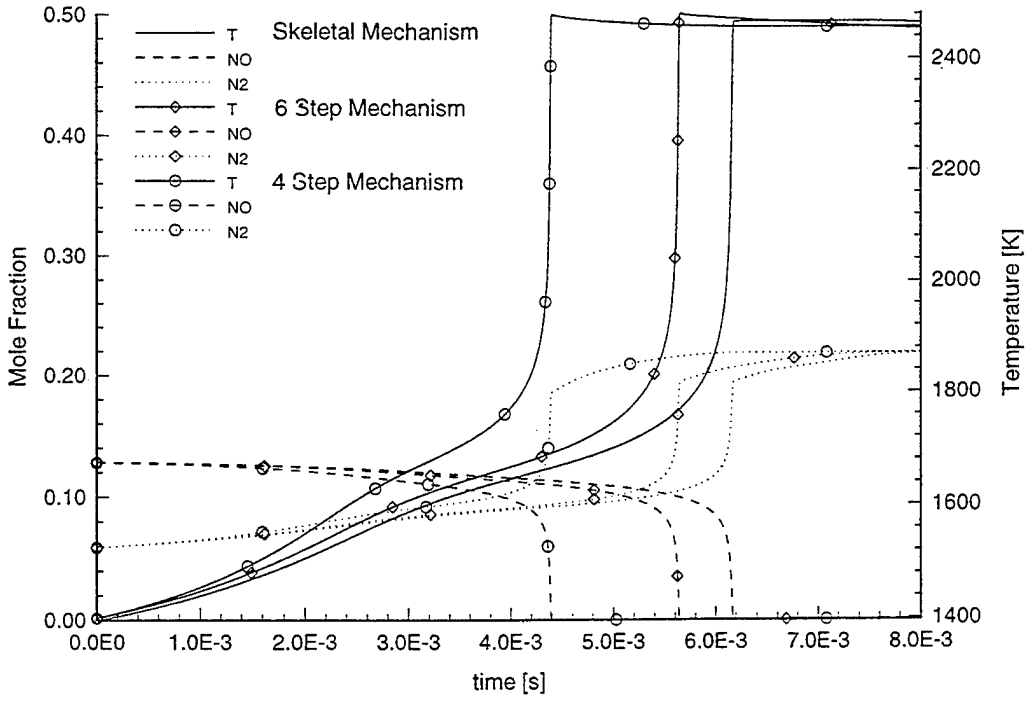

Figure 4. Profiles of temperature (T) and mole fractions of NO and N_2 plotted as a function of time. The calculations are performed using the skeletal mechanism and the reduced six-step and four-step mechanism for nitramine propellents for p = 10 atm and T^0 = 1,400 K.

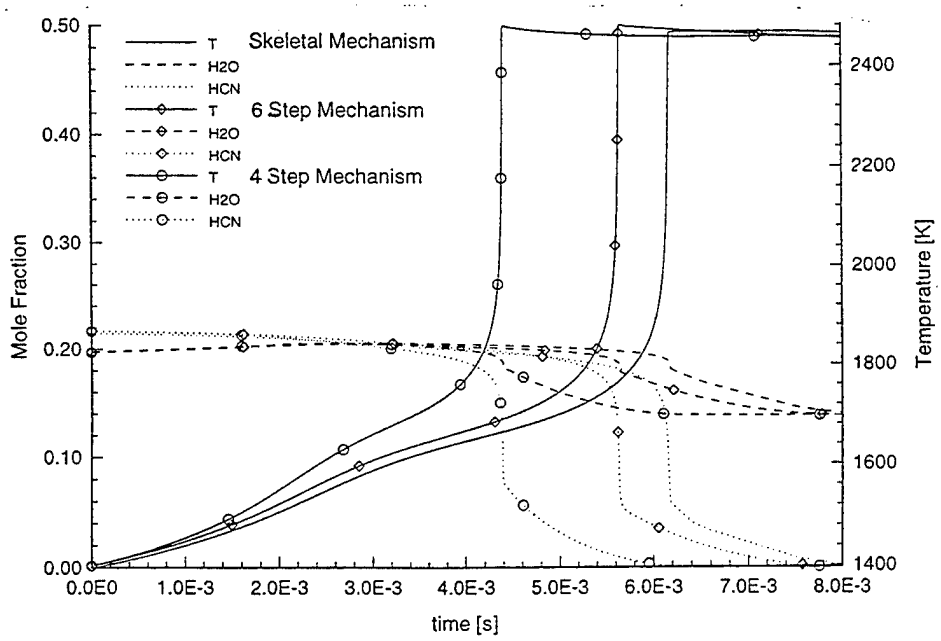

Figure 5. Profiles of temperature (T) and mole fractions of H_2O and HCN plotted as a function of time. The calculations are performed using the skeletal mechanism and the reduced six-step and four-step mechanism for nitramine propellents for p = 10 atm and T^0 = 1,400 K.

Table 3. Comparison of the Values of the Ignition Delay Times (τ_{ig}) Calculated Using the Various Mechanisms for Nitramine Propellents

Initial Conditions (atm; K)	Detailed Mechanism (41 sp., 190 r.) (s)	Skeletal Mechanism (17 sp., 23 r.) (s)	Reduced Mechanism (6 steps) (s)	Reduced Mechanism (4 steps) (s)
1;1,000	17.20	17.34	16.92	16.60
1; 1,400	$2.062 \cdot 10^{-2}$	$1.995 \cdot 10^{-2}$	$1.790 \cdot 10^{-2}$	$1.322 \cdot 10^{-2}$
1; 1,800	$3.056 \cdot 10^{-4}$	$2.602 \cdot 10^{-4}$	$2.160 \cdot 10^{-4}$	$1.319 \cdot 10^{-4}$
10; 1,000	2.754	2.265	2.185	2.171
10; 1,400	$5.723 \cdot 10^{-3}$	$6.162 \cdot 10^{-3}$	$5.632 \cdot 10^{-3}$	$4.388 \cdot 10^{-3}$
10; 1,800	$7.573 \cdot 10^{-5}$	$6.669 \cdot 10^{-5}$	$5.590 \cdot 10^{-5}$	$3.066 \cdot 10^{-5}$
30; 1,000	1.241	1.145	1.099	1.103
30; 1,400	$3.122 \cdot 10^{-3}$	$3.283 \cdot 10^{-3}$	$3.037 \cdot 10^{-3}$	$2.492 \cdot 10^{-3}$
30; 1,800	$4.903 \cdot 10^{-5}$	$4.474 \cdot 10^{-5}$	$3.803 \cdot 10^{-5}$	$2.125 \cdot 10^{-5}$

Note: The initial mole fractions of NO, CO, H_2, N_2, H_2O, CO_2, N_2O, and HCN are set equal to 0.13, 0.22, 0.07, 0.06, 0.20, 0.09, 0.02, and 0.22, respectively.

calculated using the reduced six-step mechanism agree very well with those calculated using the skeletal mechanism. The differences are less than 18%. However, the maximum differences in the values of τ_{ig} calculated using the reduced four-step mechanism and the skeletal mechanism are about 50%. The large differences between the values of τ_{ig} calculated using the reduced four-step mechanism and the skeletal mechanism are attributed to inaccuracies introduced by the steady-state approximations for H and HNCO.

Pyrolysis experiments have demonstrated that lower temperatures favor production of CH_2O and N_2O, while higher temperatures cause more HCN and NO_2 to be formed for nitramines and nitramine propellents [17, 18]. Clearly, the former intermediates reacting near the propellent surface are expected to favor formation of N_2 and N_2O at the leading edge of the dark zone, while the latter favor NO. Because a higher initial dark-zone temperature would be expected to

produce a steeper temperature gradient near the propellent surface, temperatures near the high end of the range studied might lead to initial dark-zone mixtures that contain little N_2O. Therefore, it was deemed prudent to ensure that if future experimental data exhibiting this trend become available, the reduced mechanisms would still properly predict the chemical behavior for such mixtures. For this reason, τ_{ig} calculations for an initial temperature of 1,800 K were repeated with N_2O removed from the initial mixture. The results are shown in Table 4. The differences in the values of τ_{ig} calculated using the skeletal mechanism and the six-step reduced mechanism are less than 17%, and the maximum difference in the values of τ_{ig} calculated using the skeletal mechanism and the four-step reduced mechanism is about 60%.

Table 4. Comparison of the Values of the Ignition Delay Times (τ_{ig}) Calculated Using the Various Mechanisms for Nitramine Propellents

Initial Conditions (atm; K)	Detailed Mechanism (41 sp., 190 r.) (s)	Skeletal Mechanism (17 sp., 23 r.) (s)	Reduced Mechanism (6 steps) (s)	Reduced Mechanism (4 steps) (s)
1; 1,800	$2.035 \cdot 10^{-3}$	$1.446 \cdot 10^{-3}$	$1.204 \cdot 10^{-3}$	$5.738 \cdot 10^{-4}$
10; 1,800	$5.858 \cdot 10^{-4}$	$5.233 \cdot 10^{-4}$	$4.452 \cdot 10^{-4}$	$3.026 \cdot 10^{-4}$
30; 1,800	$3.270 \cdot 10^{-4}$	$3.090 \cdot 10^{-4}$	$2.671 \cdot 10^{-4}$	$1.944 \cdot 10^{-4}$

Note: The initial mole fractions of NO, CO, H_2, N_2, H_2O, CO_2, and HCN are set equal to 0.133, 0.224, 0.071, 0.061, 0.204, 0.091, and 0.224, respectively.

The data in Tables 3 and 4 highlight the importance of the trace of N_2O in the initial mixture. Comparison of results in these tables shows that, in general, the presence of the N_2O decreases τ_{ig} by nearly a factor of 2 at 1,800 K. The effect is even greater at lower temperatures (not shown). Addition of N_2O to the mixtures results in an increase in the rate of the reaction $N_2O + M = N_2 + O + M$ (Table 1, elementary step 1), an important radical source.

5. SUMMARY AND CONCLUSIONS

Skeletal and reduced chemical-kinetic mechanisms are derived for predicting the structure of the dark zones formed over the burning surface of typical double-base and nitramine propellents. In the calculations with the reduced mechanisms, the final mass fractions of the atoms after ignition differ from their initial values because the concentrations of the steady-state species are not included in the atom conservation equations. Therefore, the reduced mechanisms are suitable for calculating the values of τ_{ig}, but in some applications, the errors introduced in the final temperature and species' concentrations may not be acceptable. Attempts to improve the accuracy of the predictions of the final concentrations of these species in the reduced mechanisms are in progress. It is hoped that these skeletal and reduced chemical-kinetic mechanisms will be suitable for use in interior ballistics calculations.*

* Recently, we have performed further updates to the detailed chemical mechanism from which the skeletal and reduced mechanisms are derived. We have discovered that three important reactions involving two additional species were overlooked for the detailed mechanism. These changes have pronounced effects at low temperatures, especially at high pressures, resulting in shortening of predicted ignition delays by up to a factor of 3. The effects are, unfortunately, negligible in regions where experimental data are available for testing. Reduced mechanisms have been developed from the newest detailed mechanism in a way entirely analogous to that used herein. The results are qualitatively similar in terms of accuracy compared to the detailed mechanism. The number of reactions in both skeletal mechanisms increases by three and the steady-state species increase by two. These new results, as well as comparisons to our previous results, will be presented in future reports.

INTENTIONALLY LEFT BLANK.

6. REFERENCES

1. Kooker, D. E., L. M. Chang, and S. L. Howard. "Flamespreading in Granular Solid Propellant. Design of an Experiment." ARL-TR-80, U.S. Army Research Laboratory, Aberdeen Proving Ground, MD, June 1993.

2. Kooker, D. E., L. M. Chang, and S. L. Howard. "Flamespreading in Granular Solid Propellant. Initial Results." ARL-TR-446, U.S. Army Research Laboratory, Aberdeen Proving Ground, MD, June 1994.

3. Kooker, D. E., L. M. Chang, and S. L. Howard. "Flamespreading in Granular Solid Propellant. Influence of Propellant Composition." 32nd JANNAF Combustion Subcommittee Meeting, Huntsville, AL, October 1995.

4. Kooker, D. E. Private communication, U.S. Army Research Laboratory, Aberdeen Proving Ground, MD, 1995.

5. Fifer, R. A., A. J. Kotlar, M. S. Miller, and J. B. Morris. "Dark Zone Modeling for Delayed Ignition Kinetics." 27th JANNAF Combustion Subcommittee Meeting, vol. I, CPIA Publication 557, p. 95, 1990.

6. Vanderhoff, J. A., W. R. Anderson, and A. J. Kotlar. "Dark Zone Modeling of Solid Propellant Flames." 29th JANNAF Combustion Subcommittee Meeting, vol. II, CPIA Publication 593, p. 225, 1992.

7. Anderson, W. R., N. Ilincic, and K. Seshadri. "Studies of Reactions Pertaining to and Development of a Reduced Mechanism for the Double Base Propellant Dark Zone." 31st JANNAF Combustion Subcommittee Meeting, vol. II, CPIA Publication 620, p. 387, 1994.

8. Anderson, W. R., N. Ilincic, N. E. Meagher, K. Seshadri, and J. A. Vanderhoff. "Detailed and Reduced Chemical Mechanisms for the Dark Zones of Double-Base and Nitramine Propellants in the Intermediate Temperature Regime." 32nd JANNAF Combustion Subcommittee Meeting, vol. 1, CPIA Publication 638, p. 197, Huntsville, AL, October 1995.

9. Anderson, W. R., N. Ilincic, N. E. Meagher, K. Seshadri, and J. A. Vanderhoff. "Chemical Kinetic Mechanisms for Characterizing the Structure of the Dark Zone of Double-Base and Nitramine Propellants." Paper in Preparation, 1996.

10. Tsang, W. and J. T. Herron. "Chemical Kinetic Database for Propellant Combustion. I. Reactions Involving NO, NO_2 , HNO, HNO_2, HCN, and N_2O." Journal of Physical and Chemical Reference Data, vol. 20, p. 609, 1991.

11. Heller, C. A. and A. S. Gordon. "Structure of the Gas Phase Combustion Region of a Solid Propellant." Journal of Physical Chemistry, vol. 59, p. 773, 1955.

12. Lutz, A. E., R. J. Kee, and J. A. Miller. "SENKIN: A FORTRAN Program for Predicting Homogeneous Gas Phase Chemical Kinetics with Sensitivity Analysis." TR-SAND87-8248, Sandia National Laboratories, October, 1988.

13. Anderson, W. R., S. W. Haga, J. F. Nuzman, and A. J. Kotlar. To be published.

14. Peters, N. "Reducing Mechanisms." M. D. Smooke, editor. Reduced Kinetic Mechanisms and Asymptotic Approximations for Methane-Air Flames, vol. 384, Lecture Notes in Physics, Springer-Verlag, Berlin Heidelberg, ch. 3, pp. 48–67, 1991.

15. Göttgens, J., and P. Terhoeven. "RedMech-an Automatic Reduction Program." N. Peters and B. Rogg, editors. Reduced Kinetic Mechanisms for Applications in Combustion Systems, vol. 15, Lecture Notes in Physics, Springer-Verlag, Berlin Heidelberg, pp. 345–349, 1993.

16. Williams, F. A. Combustion Theory. Addison-Wesley Publishing Company, Redwood City, CA, pp. 565–570, 1985.

17. Fifer, R. A. "Chemistry of Nitrate Ester and Nitramine Propellants." In K. K. Kuo and M. Summerfield, editors. Fundamentals of Solid-Propellant Combustion, vol. 90, Progress in Astronautics and Aeronautics, American Institute of Aeronautics and Astronautics, New York, pp. 177–237, 1984.

18. Schroeder M. A. "Critical Analysis of Nitramine Decomposition Data: Product Distributions From HMX and RDX Decomposition." TR-BRL-2659, AD-A159 325, U.S. Army Research Laboratory, Aberdeen Proving Grounds, MD, June 1985. (See also Proceedings, 18th JANNAF Combustion Meeting, CPIA Publication 347, vol. II, pp. 395–413, Pasadena, CA, October, 1981.)

NO. OF COPIES	ORGANIZATION
2	DEFENSE TECHNICAL INFORMATION CENTER DTIC DDA 8725 JOHN J KINGMAN RD STE 0944 FT BELVOIR VA 22060-6218
1	HQDA DAMO FDQ DENNIS SCHMIDT 400 ARMY PENTAGON WASHINGTON DC 20310-0460
1	CECOM SP & TRRSTRL COMMCTN DIV AMSEL RD ST MC M H SOICHER FT MONMOUTH NJ 07703-5203
1	PRIN DPTY FOR TCHNLGY HQ US ARMY MATCOM AMCDCG T M FISETTE 5001 EISENHOWER AVE ALEXANDRIA VA 22333-0001
1	PRIN DPTY FOR ACQUSTN HQS US ARMY MATCOM AMCDCG A D ADAMS 5001 EISENHOWER AVE ALEXANDRIA VA 22333-0001
1	DPTY CG FOR RDE HQS US ARMY MATCOM AMCRD BG BEAUCHAMP 5001 EISENHOWER AVE ALEXANDRIA VA 22333-0001
1	ASST DPTY CG FOR RDE HQS US ARMY MATCOM AMCRD COL S MANESS 5001 EISENHOWER AVE ALEXANDRIA VA 22333-0001

NO. OF COPIES	ORGANIZATION
1	DPTY ASSIST SCY FOR R&T SARD TT F MILTON THE PENTAGON RM 3E479 WASHINGTON DC 20310-0103
1	DPTY ASSIST SCY FOR R&T SARD TT D CHAIT THE PENTAGON WASHINGTON DC 20310-0103
1	DPTY ASSIST SCY FOR R&T SARD TT K KOMINOS THE PENTAGON WASHINGTON DC 20310-0103
1	DPTY ASSIST SCY FOR R&T SARD TT B REISMAN THE PENTAGON WASHINGTON DC 20310-0103
1	DPTY ASSIST SCY FOR R&T SARD TT T KILLION THE PENTAGON WASHINGTON DC 20310-0103
1	OSD OUSD(A&T)/ODDDR&E(R) J LUPO THE PENTAGON WASHINGTON DC 20301-7100
1	ARL ELECTROMAG GROUP CAMPUS MAIL CODE F0250 A TUCKER UNIVERSITY OF TX AUSTIN TX 78712
1	DUSD SPACE 1E765 J G MCNEFF 3900 DEFENSE PENTAGON WASHINGTON DC 20301-3900
1	USAASA MOAS AI W PARRON 9325 GUNSTON RD STE N319 FT BELVOIR VA 22060-5582

NO. OF COPIES	ORGANIZATION
1	CECOM PM GPS COL S YOUNG FT MONMOUTH NJ 07703
1	GPS JOINT PROG OFC DIR COL J CLAY 2435 VELA WAY STE 1613 LOS ANGELES AFB CA 90245-5500
1	ELECTRONIC SYS DIV DIR CECOM RDEC J NIEMELA FT MONMOUTH NJ 07703
3	DARPA L STOTTS J PENNELLA B KASPAR 3701 N FAIRFAX DR ARLINGTON VA 22203-1714
1	SPCL ASST TO WING CMNDR 50SW/CCX CAPT P H BERNSTEIN 300 O'MALLEY AVE STE 20 FALCON AFB CO 80912-3020
1	USAF SMC/CED DMA/JPO M ISON 2435 VELA WAY STE 1613 LOS ANGELES AFB CA 90245-5500
1	US MILITARY ACADEMY MATH SCI CTR OF EXCELLENCE DEPT OF MATHEMATICAL SCI MDN A MAJ DON ENGEN THAYER HALL WEST POINT NY 10996-1786
1	DIRECTOR US ARMY RESEARCH LAB AMSRL CS AL TP 2800 POWDER MILL RD ADELPHI MD 20783-1145

NO. OF COPIES	ORGANIZATION
1	DIRECTOR US ARMY RESEARCH LAB AMSRL CS AL TA 2800 POWDER MILL RD ADELPHI MD 20783-1145
3	DIRECTOR US ARMY RESEARCH LAB AMSRL CI LL 2800 POWDER MILL RD ADELPHI MD 20783-1145
	ABERDEEN PROVING GROUND
2	DIR USARL AMSRL CI LP (305)

NO. OF COPIES	ORGANIZATION
2	UNIVERSITY OF CALIFORNIA AT SAN DIEGO DEPT OF APPLIED MECH & ENGRNG SCIENCE ATTN K SESHADRI LA JOLLA CA 92093-0411

NO. OF COPIES	ORGANIZATION
	ABERDEEN PROVING GROUND
41	DIR, USARL ATTN: AMSRL-WM-P, A. W. HORST AMSRL-WM-PC, B. E. FORCH G. F. ADAMS W. R. ANDERSON R. A. BEYER S. W. BUNTE C. F. CHABALOWSKI K. P. MCNEILL-BOONSTOPPEL A. COHEN R. CUMPTON R. DANIEL D. DEVYNCK R. A. FIFER J. M. HEIMERL B. E. HOMAN A. JUHASZ A. J. KOTLAR R. KRANZE E. LANCASTER W. F. MCBRATNEY K. L. MCNESBY M. MCQUAID N. E. MEAGHER M. S. MILLER A. W. MIZIOLEK J. B. MORRIS J. E. NEWBERRY S. V. PAI R. A. PESCE-RODRIGUEZ J. RASIMAS P. REEVES B. M. RICE P. SAEGAR R. C. SAUSA M. A. SCHROEDER R. SCHWEITZER L. D. SEGER J. A. VANDERHOFF D. VENIZELOS A. WHREN H. L. WILLIAMS

INTENTIONALLY LEFT BLANK.

REPORT DOCUMENTATION PAGE

Form Approved
OMB No. 0704-0188

1. AGENCY USE ONLY *(Leave blank)*	2. REPORT DATE	3. REPORT TYPE AND DATES COVERED
	May 97	Final, February 1994 - July 1996

4. TITLE AND SUBTITLE

Reduced Chemical-Kinetic Mechanisms for the Dark Zones of Double-Base and Nitramine Gun Propellents

5. FUNDING NUMBERS

PR: 1L161102AH43

6. AUTHOR(S)

N. Ilincic, K. Seshadri, W. R. Anderson, and N. E. Meagher

7. PERFORMING ORGANIZATION NAME(S) AND ADDRESS(ES)

U.S. Army Research Laboratory
ATTN: AMSRL-WM-PC
Aberdeen Proving Ground, MD 21005-5066

8. PERFORMING ORGANIZATION REPORT NUMBER

ARL-TR-1352

9. SPONSORING/MONITORING AGENCY NAMES(S) AND ADDRESS(ES)

10.SPONSORING/MONITORING AGENCY REPORT NUMBER

11. SUPPLEMENTARY NOTES

12a. DISTRIBUTION/AVAILABILITY STATEMENT

Approved for public release; distribution is unlimited.

12b. DISTRIBUTION CODE

13. ABSTRACT *(Maximum 200 words)*

Simplified chemical-kinetic mechanisms were employed to calculate the structure of the dark zones of burning double-base and nitramine propellants. These reduced mechanisms are expected to be useful in interior ballistic calculations. First, skeletal mechanisms comprised of 22 elementary reactions among 15 species and 23 elementary reactions among 17 species were used to calculate dark zone structures for double-base and nitramine propellants, respectively. The skeletal mechanisms were previously extracted from a detailed mechanism incorporating 190 elementary reactions involving 41 species. Ignition delay times (τ_{ig}) were calculated for homogeneous mixtures in which the initial concentrations of reactants were similar to those found at the beginning of propellent dark zones. The τ_{ig} calculations were performed for various initial pressures and temperatures. The τ_{ig} calculated using the skeletal and detailed mechanisms agreed well. Reduced mechanisms were derived from the skeletal mechanisms by introducing steady-state approximations for a number of species. For double-base propellants, a reduced mechanism of three global reactions was obtained. Reduced mechanisms utilizing six and four global reactions were deduced for nitramine propellants. The τ_{ig} and structures of the dark zones calculated using the reduced three-step mechanism for double-base propellants and six-step mechanism for nitramine propellants were in agreement with calculations made using the skeletal mechanisms. Agreement using the four-step reduced mechanism for nitramine propellants was not good; however, it might still be useful for some applications.

14. SUBJECT TERMS

combustion, propellant chemistry, kinetic mechanisms, propellant dark zone

15. NUMBER OF PAGES

26

16. PRICE CODE

17. SECURITY CLASSIFICATION OF REPORT	18. SECURITY CLASSIFICATION OF THIS PAGE	19. SECURITY CLASSIFICATION OF ABSTRACT	20. LIMITATION OF ABSTRACT
UNCLASSIFIED	UNCLASSIFIED	UNCLASSIFIED	UL

INTENTIONALLY LEFT BLANK.

USER EVALUATION SHEET/CHANGE OF ADDRESS

This Laboratory undertakes a continuing effort to improve the quality of the reports it publishes. Your comments/answers to the items/questions below will aid us in our efforts.

1. ARL Report Number/Author ARL-TR-1352 (Ilincic [POC: Anderson]) Date of Report May 1997

2. Date Report Received _____

3. Does this report satisfy a need? (Comment on purpose, related project, or other area of interest for which the report will be used.) _____

4. Specifically, how is the report being used? (Information source, design data, procedure, source of ideas, etc.) _____

5. Has the information in this report led to any quantitative savings as far as man-hours or dollars saved, operating costs avoided, or efficiencies achieved, etc? If so, please elaborate. _____

6. General Comments. What do you think should be changed to improve future reports? (Indicate changes to organization, technical content, format, etc.) _____

CURRENT ADDRESS

_____
Organization

_____
Name E-mail Name

_____
Street or P.O. Box No.

_____
City, State, Zip Code

7. If indicating a Change of Address or Address Correction, please provide the Current or Correct address above and the Old or Incorrect address below.

OLD ADDRESS

_____
Organization

_____
Name

_____
Street or P.O. Box No.

_____
City, State, Zip Code

(Remove this sheet, fold as indicated, tape closed, and mail.)

(DO NOT STAPLE)

DEPARTMENT OF THE ARMY

OFFICIAL BUSINESS

NO POSTAGE
NECESSARY
IF MAILED
IN THE
UNITED STATES

BUSINESS REPLY MAIL
FIRST CLASS PERMIT NO 0001,APG,MD

POSTAGE WILL BE PAID BY ADDRESSEE

DIRECTOR
US ARMY RESEARCH LABORATORY
ATTN AMSRL WM PC
ABERDEEN PROVING GROUND MD 21005-5066